Oil & Natural Gas Technology

DOE Award No.: DE-FE 0009963

Quarterly Research Performance Progress Report (Period ending 09/30/2014)

Measurement and Interpretation of Seismic Velocities and Attenuations in Hydrate-Bearing Sediments

Project Period (10/1/2012 to 9/30/2015)

Submitted by:
PI: Michael Batzle
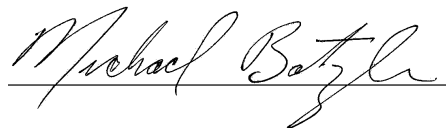Colorado School of Mines
DUNS #010628170.
1500 Illinois Street
Golden. CO 80401
e-mail: mbatzle@mines.edu
Phone number: (303) 384-2067
Submission Date: 8/4/2014

Prepared for:
United States Department of Energy
National Energy Technology Laboratory

NETL

Office of Fossil Energy

Disclaimer:

This report was prepared as an account of work sponsored by an agency of the United States Government. Neither the United States Government nor any agency thereof, nor any of their employees, makes any warranty, express or implied, or assumes any legal liability or responsibility for the accuracy, completeness, or usefulness of any information, apparatus, product, or process disclosed, or represents that its use would not infringe privately owned rights. Reference herein to any specific commercial product, process, or service by trade name, trademark, manufacturer, or otherwise does not necessarily constitute or imply its endorsement, recommendation, or favoring by the United States Government or any agency thereof. The views and opinions of authors expressed herein do not necessarily state or reflect those of the United States Government or any agency thereof.

Abstract:

Measurement and Interpretation of Seismic Velocities and Attenuations
in Hydrate-Bearing Sediments

Grant/Cooperative Agreement DE-FE 0009963.

During this period we focused on measurements of elastic wave velocity and attenuation in hydrate-bearing sediments. Several publications have indicated increasing attenuation with increasing hydrate content. As part of this research, methane hydrates were grown in sand packs using the split Hopkinson bar apparatus at the Lawrence Berkeley National laboratory. In addition, measurements were also made for samples containing CO_2 and N_2 hydrates. Pure THF hydrates were also measured to establish the expected background attenuation.

- With formation of hydrates, typically velocities and moduli increase (as expected)

- However, if hydrate formation is heterogeneous and forms in a few clumps, the velocity is not sensitive to the hydrate formation.

- Attenuation increases substantially with increasing hydrate content when slightly above $0^{o}C$.

- Similarly, both velocity and attenuation increase with formation of CO_2 / N_2 hydrates

- For pure THF, attenuation also increases when near $0^{o}C$ and hydrate is formed.

- For pure THF at much lower temperatures, attenuation decreases.

The increase in attenuation is likely due to residual liquid water either within the hydrate crystal framework or clinging to the mineral surfaces. This is consistent with the loss of attenuation at lower temperatures where the remaining liquid water turns to ice.

Contents:

Figures and Tables:

Executive Summary:

This project is to measure seismic velocities and attenuations under known saturations and textural conditions. This information is needed to calibrate estimates of hydrate saturation from surface seismic data. During this quarter, we performed measurements of elastic properties and attenuation on a gas-hydrate bearing sand pack. Many of the measurements were made at the Lawrence Berkeley National Laboratory with Tim Kneafsey and Seiji Nakagawa. We greatly appreciate their efforts.

The observed increase in Young's modulus and shear modulus as well as compressional and shear wave velocities indicate an increase in mechanical stiffness due to methane hydrate formation. The sand pack's stiffness increases as methane hydrate works as a cement between grains in the pore space. During the hydrate formation process most of the water is consumed resulting in an attenuation decrease and a stabilization of attenuation at a higher value than before the hydrate formation. The behavior of attenuation upon methane hydrate formation may be explained by squirt flow in the pore space: due to hydrate formation remaining pore water is pushed towards the grain surfaces and contacts resulting in higher attenuation.

Direct observation shows that methane hydrate forms patchy, inhomogeneous distributions, even when the initial water distribution in the sample's pore space is homogeneous. The delay in response of the resonant bar data upon initial hydrate formation indicates that this patchy saturation may not always be detected by mechanical measurements. When one distinct body of methane hydrate was present in the sand pack no significant increase in elastic moduli and attenuation was visible. Only after the methane hydrate diffused throughout the sample did an increase in elastic moduli and attenuation became apparent. Thus, discreet bodies of methane hydrate in natural sediment may not always be detectable in seismic surveys.

The stiffness of the sand pack decreased when part of the methane hydrate was dissociated leaving the pore space filled with water, methane gas and methane hydrate. The effect of the partial dissociation on attenuation cannot be interpreted in detail since both shear and extensional attenuation were altered by the inhomogeneous distributions. An attenuation increases may be attributed to the increase in water saturation due to hydrate dissociation. After the initial increase, attenuation decreases to approximately the same value as before in the sample with near complete hydrate conversion.

During the last stage of the experiment, the injection of CO_2 and N_2 gas into three phase system, we observed an increase in stiffness. The values for elastic moduli and shear and compressional velocities increased but to lower values than observed before in the pure methane-hydrate bearing sample after full conversion of all pore water. The comparably low stiffness of the sample indicates that not all pore water was converted to hydrate by the time the blockage occurred. The CT images during that stage of the experiment show that gas hydrate formed mostly along the less dense areas of the layered. This observation indicates that gas hydrate preferentially forms in areas of higher porosity. The attenuation increases initially which again may be related to a water film and squirt flow.

To address the possibility of hydrates themselves being "lossy" or low Q materials direct measurements of ultrasonic wave propagation were also conducted on a tetrahydrofuran (THF) hydrate. At temperatures close to 0°C, the THF hydrate sample had high attenuation, or was very lossy. However, on further cooling, the attenuation diminished, suggesting again that residual liquid water is responsible for losses and at lower temperatures, water turns to ice and attenuation significantly decreases.

Accomplishments

Split-Hopkinson Bar Measurements

We conducted Split-Hopkinson resonant bar measurements on a gas hydrate bearing sand pack to determine the material mechanical properties. Young's modulus, shear modulus, compressional and shear velocities as well as corresponding attenuations were measured during methane hydrate formation, partial dissociation of methane hydrate and injection of CO2 and N2 gas to replace methane gas in the hydrate. Additionally, X-ray computed tomography was used to monitor gas hydrate distribution and saturation in the sand pack and gas chromatography was used during the gas replacement to monitor the composition of produced gas. Our measurements showed a clear influence of gas hydrate formation and dissociation on mechanical strength and attenuation. Methane hydrate presence increases stiffness and attenuation of the sample. The injection of CO2 and N2 gas was followed by an additional increase in stiffness and attenuation compared to a sand pack filled with water, methane gas and methane hydrate. The CT imaging revealed the inhomogeneous, patchy nature of gas hydrate distribution showing areas of the sample completely filled with hydrate next to areas devoid of any gas hydrate.

Gas Replacement and Acoustic Properties

We performed a gas replacement experiment of methane gas in gas hydrates with a mixture of nitrogen and carbon dioxide. The experiment was performed under similar pressure and temperature conditions as present during the Ignik Sikumi gas hydrate field trial on the north slope of Alaska. The N_2/CO_2 ratio of 23% and 77%, respectively, was the same as used during the Ignik Sikumi test. The injection of N_2 and CO_2 is one of the possible methods to produce methane gas from methane hydrate (Hester and Brewer, 2009; Schoderbek et al., 2012). While the N_2/CO_2 mixture was flowed through the methane-hydrate bearing sample, changes in the sample were monitored by Split Hopkinson resonant bar measurements and X-ray computed tomography.

Experimental Procedure

The experiment consisted of three parts:

1) We formed methane hydrate in a sand pack made of F110 Ottawa sand with 39% porosity. The pressure and temperature we used was 4.83 MPa and 3.9^{o}C. This pressure-temperature combination is well above equilibrium conditions for methane hydrate (Figure 1) and was chosen to ensure close to complete conversion of water and methane to gas hydrate. We allowed 80 hours for this initial phase of the experiment.

2) To obtain a three-phase system of water, methane hydrate, and methane gas, the pore pressure was decreased to 3.90 MPa while the temperature was kept at 3.9C (equilibrium conditions).
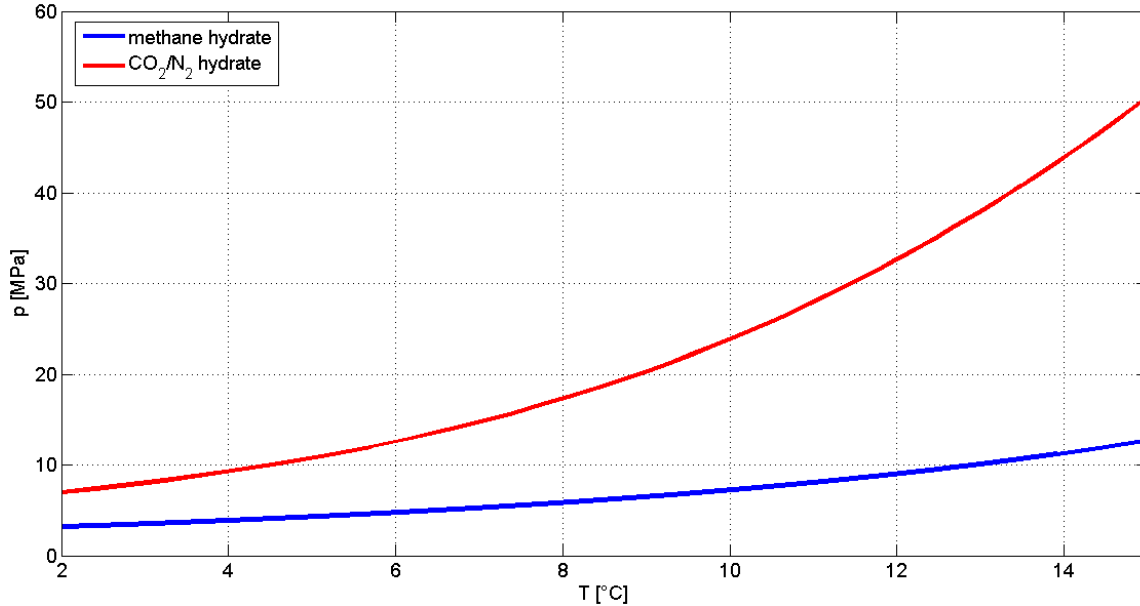
Figure 1. Stability boundaries for pure methane hydrate and hydrate of 23% carbon dioxide and 77% nitrogen modeled with CSMGem

3) A gas mixture of 23% N_2 and 77% CO_2 is flowed through the sample at 9.6 MPa. The higher pore pressure was necessary due to a higher equlibrium pressure for gas hydrate formed from the N_2-CO_2 mixture (Figure 1). During this phase of the experiment, gas samples were taken about every 15 minutes and analysed in a gas chromatograph to monitor the changing composition of the gas produced from the system.

During all three parts of the experiment the confining pressure was kept at 15.6 MPa resulting in a changing effective pressure due to pore pressure changes. Changes in hydrate saturation and distribution were monitored using X-ray computed tomography and a Split Hopkinson resonant bar apparatus (SHRB). The SHRB measures resonance frequency and dampening. This allows the measurement of mechanical properties at much lower frequencies than common ultrasonic measurements. The sonic frequency range (several hundred hertz to 10 kilohertz) is favorable over the ultrasonic range since mechanical properties of geologic materials are generally frequency dependent and the sonic range is close to frequencies employed in borehole acoustic measurements. In the conventional resonant bar method, extension and torsion mode of a long, slender sample are measured in order to determine Young's modulus and shear modulus. The resonance frequency is determined by the sample length (wavelength at resonance frequency is twice the sample length). Since rock samples are usually short, their resonance frequency is high (>10 kHz). To obtain a greater sample length and thus a lower resonance frequency, the rock sample is placed between two metal extension rods in the SHRB apparatus. In this experiment we used a 7.6 cm long sand pack placed between two stainless steel bars, each with a length of 40.6 cm. The diameter for both was 3.75 cm. Source and receiver unit are located at opposite ends of the setup (Figure 2). The measured resonance frequencies and attenuations of the whole system need to be numerically inverted to obtain moduli, velocities and attenuation of the sample only. For

details about the numerical inversion see Nakagawa (2011). Attenuation is obtained by the half power method using the following equation:

$$Q^{-1} = \Delta f / f_{res} \tag{1}$$

where Q is the seismic quality factor, Q^{-1} is the attenuation, f_{res} is the resonance frequency and Δf is the width of the resonance peak. The resonance frequency is divided by the width of the resonance peak at half of its maximum amplitude (Figure 3) to calculate the seismic quality factor Q.
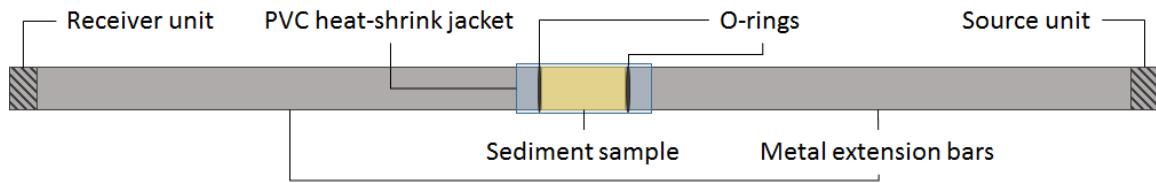

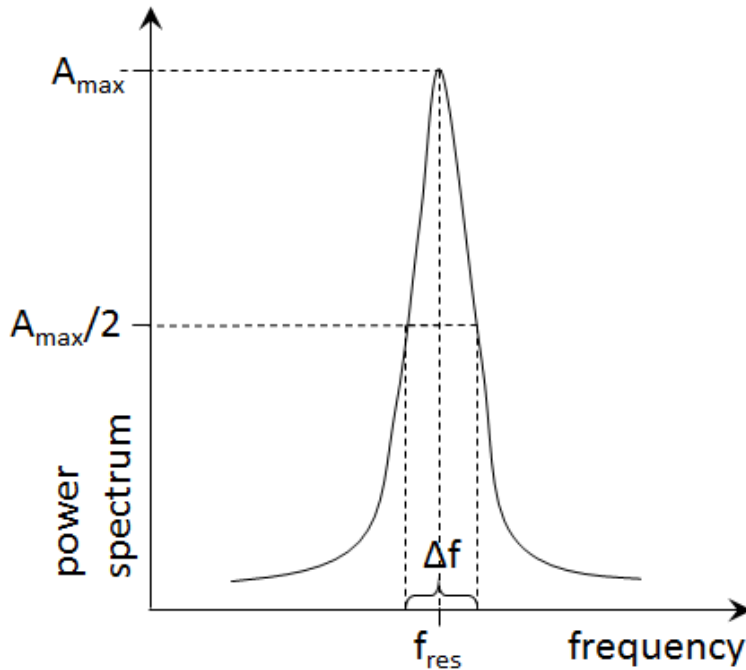Figure 2. Schematic diagram of the split Hopkinson resonant bar apparatus (SHRB)

Figure 3: Half power method to obtain seismic quality factor Q

The X-ray CT images were obtained with a medical CT scanner from General Electric (Figure 4). Image slices were acquired every 0.625 mm resulting in 144 slices for each sample. A resolution of 195 μm was used. The CT images were calibrated to density. Areas of the sample filled with gas hydrate show a higher density than areas filled with water and methane which allows us to image the distribution of the gas hydrate in the pore space. Note that methane hydrate and CO_2/N_2 hydrates have similar densities and can thus not be distinguished in CT images.

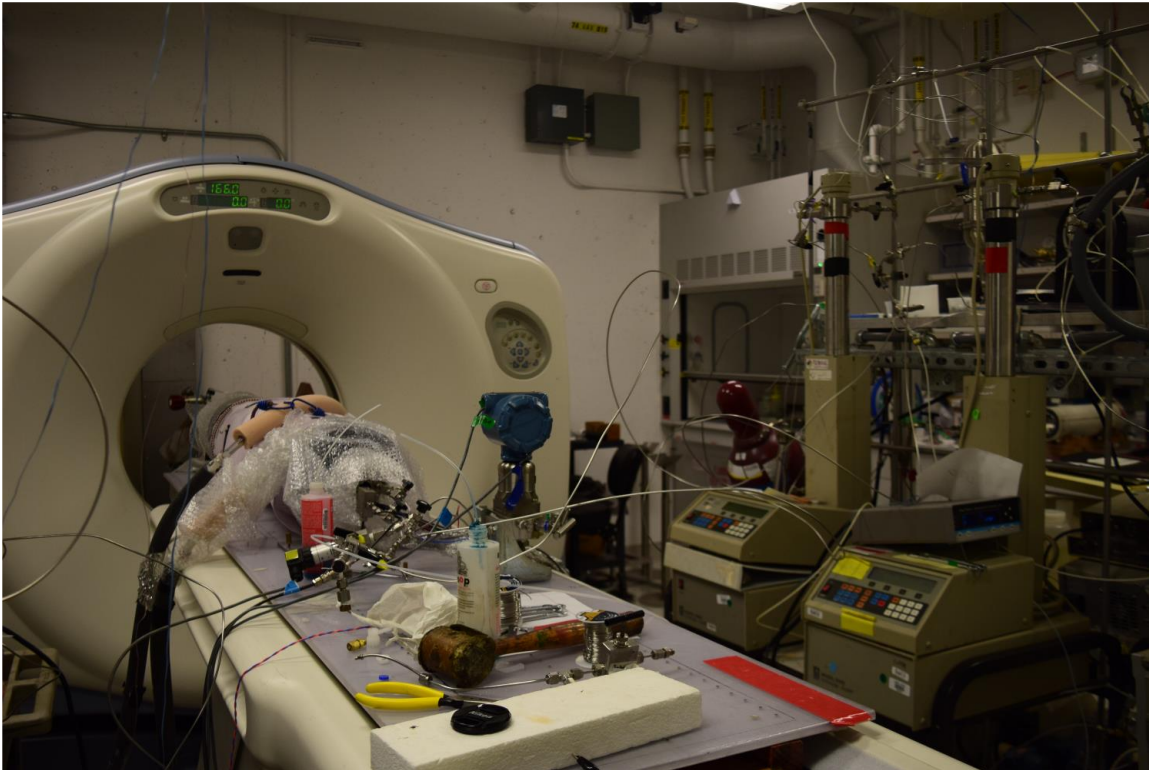

Figure 4. Equipment set-up at the Lawrence Berkley National Laboratory including CT scanner in the background.

Results

Figures 5 - 7 show the inverted resonant bar data over the course of the entire experiment. During the first 37 hours of the experiment, the sample was partially water saturated and did not contain any gas hydrates. A confining pressure cycle was performed from 0 - 1 hours after the start of the experiment. The pressure was increased from 0.34 MPa to 15.6 MPa and decreased to 0.34 MPa again. At 11.5 hours the confining pressure was permanently increased from 0.34 MPa to 15.6 MPa resulting in an increase in moduli (Figure 5), velocities (Figure 6) and Poisson's ratio (Figure 7) and a decrease in attenuation (Figures 5 and 6). After 37 hours methane gas was injected into the sample at a pore pressure of 4.83 MPa. A strong increase in moduli, velocities and Poisson's ratio and a decrease in attenuation indicated the formation of methane hydrates between 40 and 42 hours after the start of the experiment (Figures 5, 6 and 7). The pore pressure was

decreased to methane hydrate equilibrium after 109.5 hours. The partial dissociation of methane hydrate resulted in a decrease of moduli, velocities, Poission's ratio and an increase in attenuation (Figures 5, 6 and 7).

The injection of CO_2 and N_2 gas into the three-phase system of water, methane gas and methane hydrate started at 159 hours. The injection is accompanied by an increase in moduli, velocities and Poisson's ratio and a decrease in attenuation (Figures 5, 6 and 7). A hydrate blockage formed in the sample shortly after the injection of CO_2 and N_2 gas was started. The hydrate blockage caused a pore pressure gradient from the upstream end to the downstream end of the sample. In order to dissociate the blockage, the temperature of the sample was increased by 30-second heat pulses starting at 159.5 hours. Since the gas hydrate blockage could not be dissolved, temperature was increased until the end of the experiment after 211 hours. The increase in sample temperature results in a dissociation of gas hydrate in the pore space indicated by a decrease in moduli, velocities and Poisson's ratio as well as an increase in attenuation (Figures 5, 6 and 7).

For a more detailed analysis we will refer to Young's modulus and shear modulus and their corresponding attenuations since the error introduced to P- and S-wave velocities during the inversion are greater. Figure 8 shows a CT image of the partially water saturated sample. The sand is packed inhomogeneously in layers. Darker colors indicate less densely packed areas. The average density of the sample before hydrate formation was 1.8 g/cm^3.
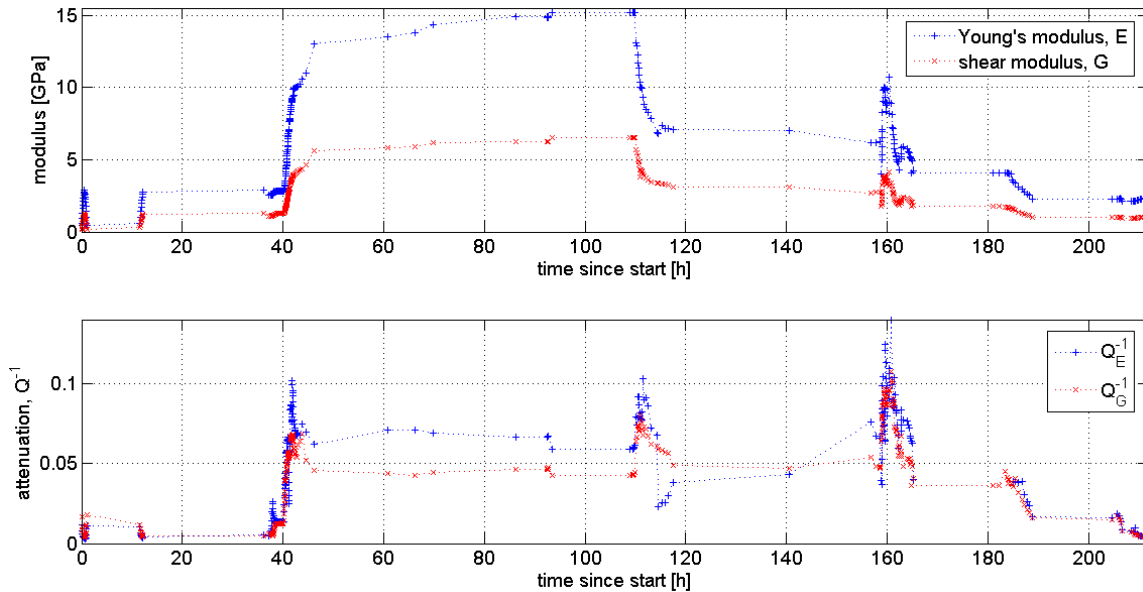

Figure 5. Inverted Young's modulus and shear modulus with corresponding attenuations from SHRB data
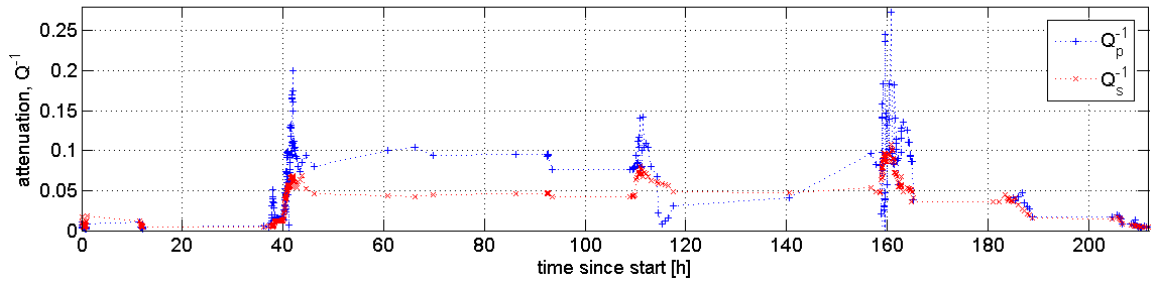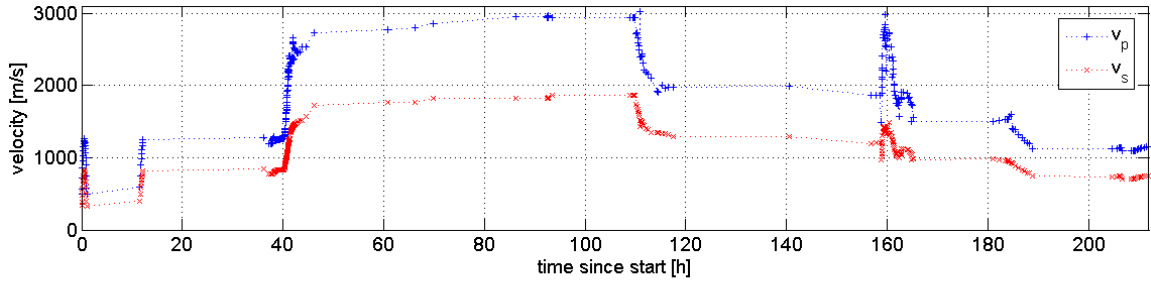
Figure 6. Inverted P- and S-wave velocities and corresponding attenuations from SHRB Data
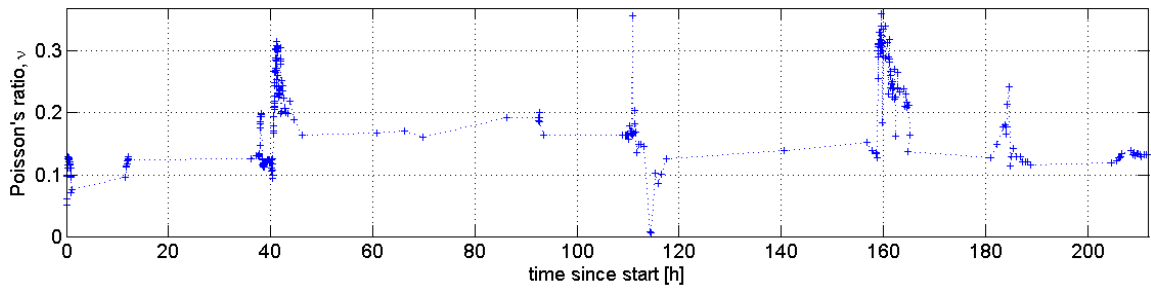
Figure 7.   Poisson's ratio obtained from inverted SHRB data

13
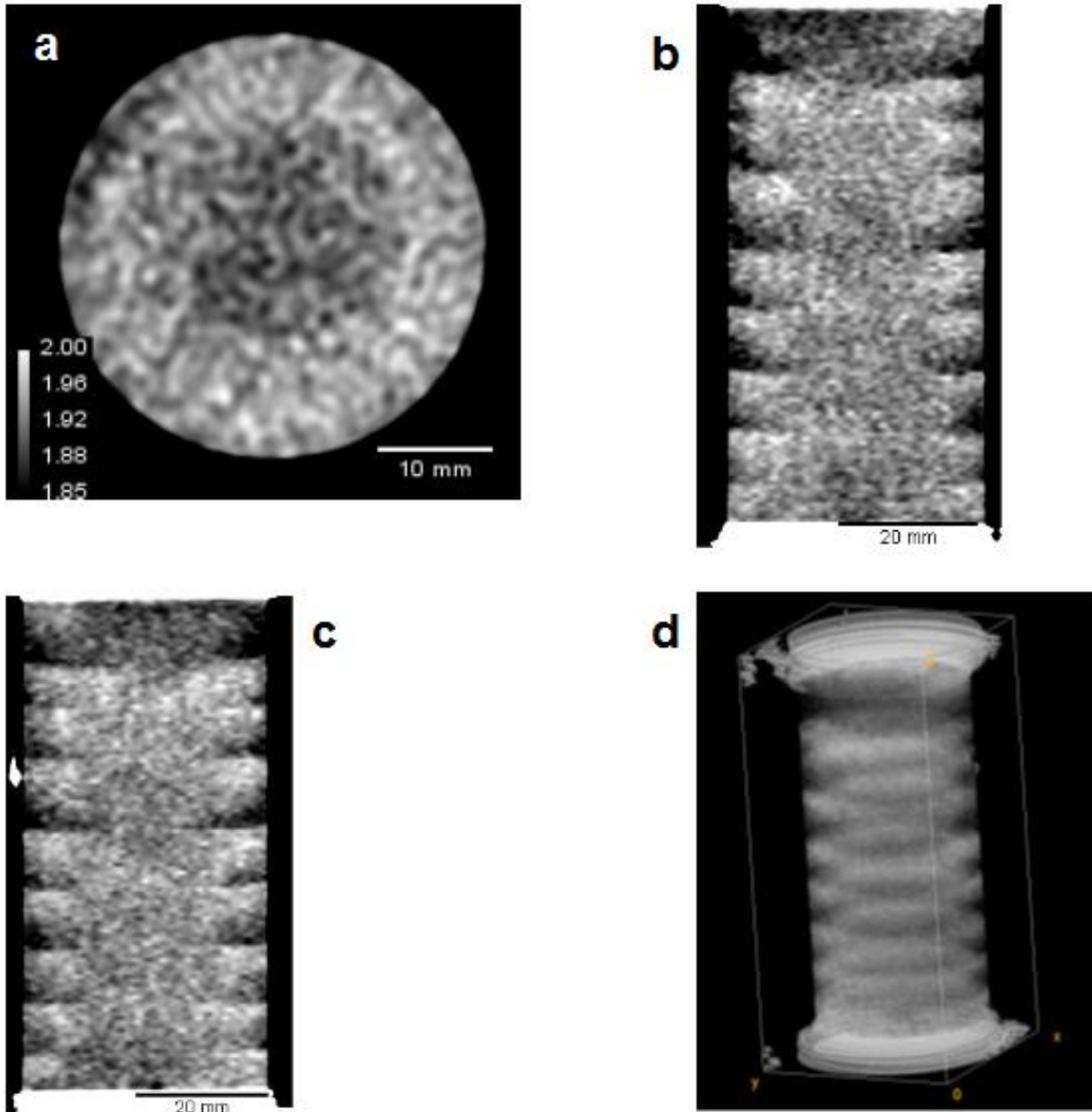
Figure 8. CT images of partially water saturated sample before hydrate formation

The CT image of the wet sample was used as a standard for further CT scans: subtracting the gray scale values (or densities) of the wet sample CT image from a CT image of a hydrate-bearing sample, results in positive and negative density differences. Positive density differences represent gas-hydrate filled sediment; negative density differences represent areas which were water-filled before and are now dry since the water has been used for gas hydrate formation.

Experimental Phase 1: Methane Hydrate Formation

After methane gas was injected into the sample 37 hours after the start of the experiment, no immediate effect was visible in the SHRB data. About 40 minutes after the methane injection started, a slight increase in Young's modulus occurs (Figure 9). An increase in extensional attenuation occurs at the same time. After the initial increase in extensional attenuation, the attenuation value decreases again but both - Young's and shear attenuation remain at a higher level. CT images taken at the same time indicate that a bulk body of methane hydrate has formed on the wall of the sample (Figure 10).

At 40.2 hours Young's modulus, shear modulus and the corresponding attenuations start to increase drastically. CT images taken at the same time indicate a movement of the hydrate-formation front from the surface of the initial hydrate body towards the opposing wall of the sample and the ends of the sample (Figure 11). The increase in both moduli continues until 42 hours and then remains at a stable value. The attenuations increase until 41.8 hours and then decrease again. Shear attenuation increases steadily whereas for extensional attenuation periods of increase and decrease occur resulting in an overall increase (Figure 9). After 42 hours no further change in CT images was visible indicating that the hydrate formation slowed significantly by that time. By the end of the methane hydrate formation process the area of the initial hydrate body appears to be free of hydrate (Figure 11).
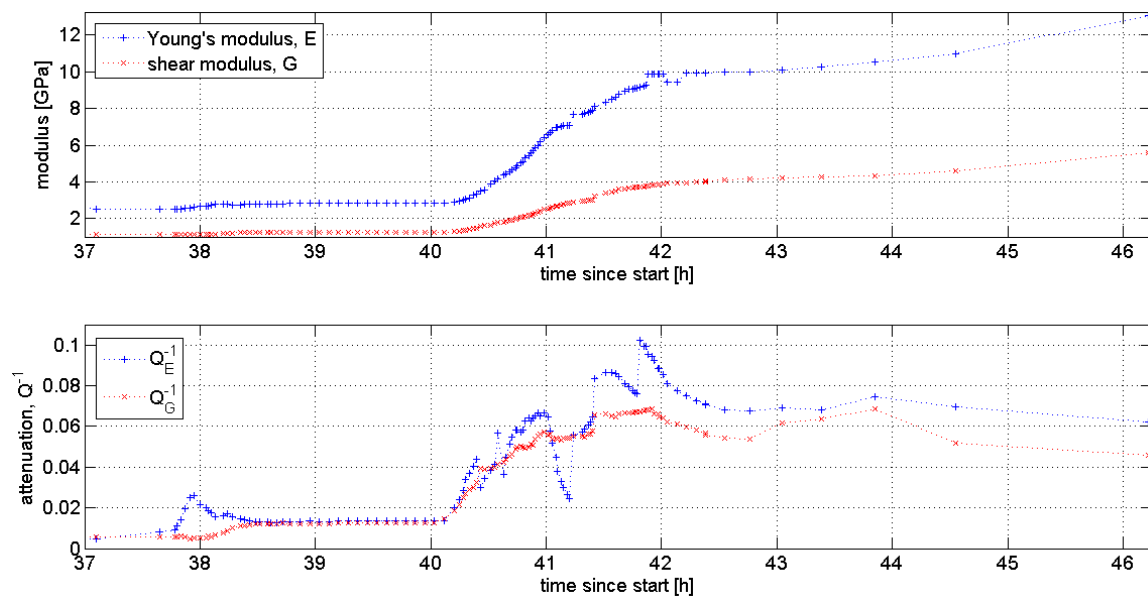
Figure 9. Inverted Young's modulus and shear modulus with corresponding attenuations from SHRB data recorded during methane hydrate formation. Methane injection was started at 37 hours; the initial methane hydrate formation lasted until approximately 42 hours.
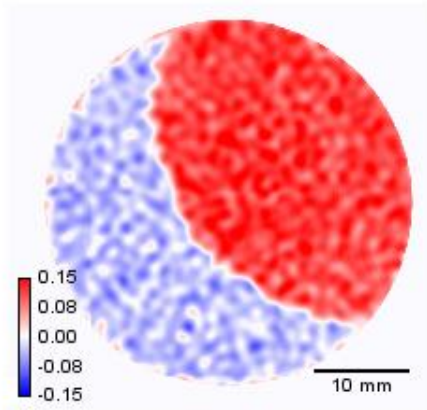
(a) xy slice
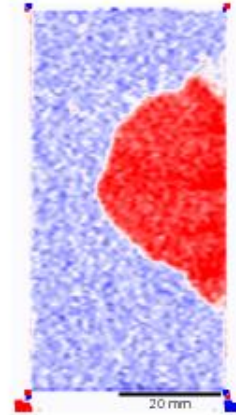
(b) xz slice
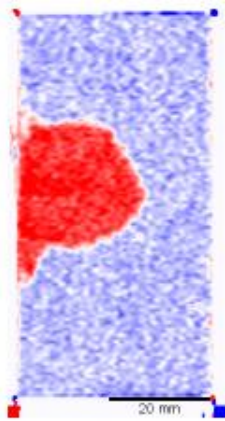
(c) yz slice
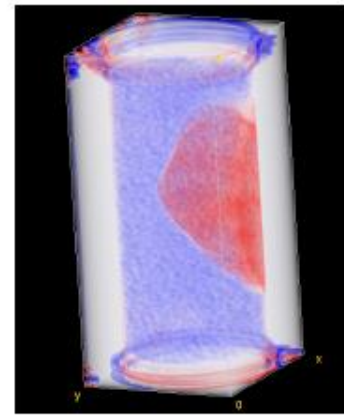
(d) 3D view

Figure 10. Change in density obtained by subtracting CT image of partially water saturated sample from CT image after initial methane hydrate formation (38 hours after start of experiment)

(a) xy slice

(b) xz slice

(c) yz slice

(d) 3D view
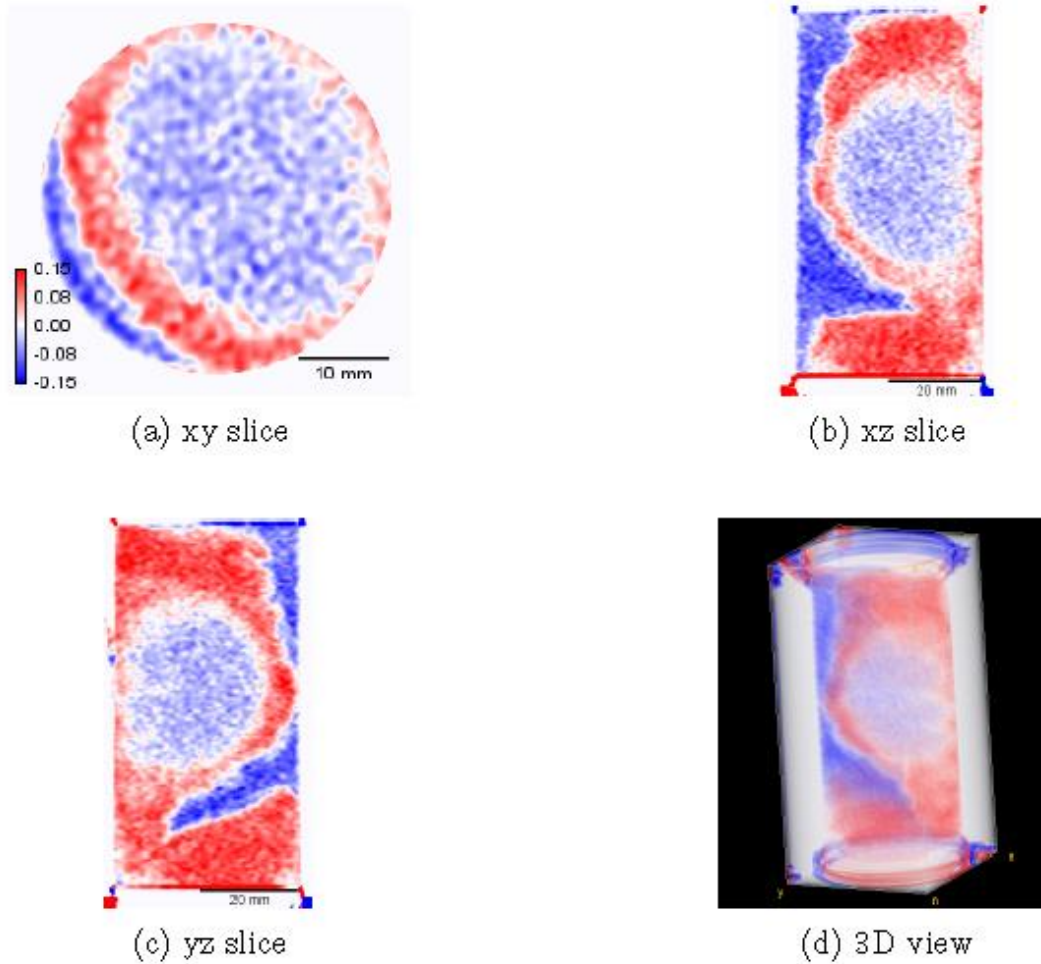
Figure 11. Change in density obtained by subtracting CT image of partially water saturated sample from CT image after continued methane hydrate formation (42 hours after experiment started)

Experimental Phase 2: Pore-Pressure Decrease to Equilibrium

After nearly all water in the pore space was converted to methane hydrate, the pore pressure was decreased from 4.82 MPa to 3.90 MPa resulting in a three phase system of methane, water and methane hydrate in the pore space. The decrease in pore pressure to methane hydrate equilibrium conditions resulted in a decrease in compressional and shear (Figure 12). The values of both moduli remain above the initial values before methane hydrate was formed indicating that there is still methane hydrate left in the pore space. The attenuations react to the decreased pore pressure with an initial increase followed by a decrease. Extensional attenuation remains at a value higher than for the hydrate-free, partially water-saturated sample but lower than the value after full conversion to methane hydrate. Shear attenuation appears to be higher than in the previous phase of the experiment (Figure 6). The extension mode resonance peak was distorted between 110.8 hours and 156.9 hours by a strong bending mode interference. The torsion mode

17

resonance frequency appeared to be split into two small peaks between 144.4 hours and 117.5 hours. This behavior is likely to cause great errors in attenuations thus the different behavior of Young's and shear attenuation in this phase of the experiment should not be interpreted.

No visible changes in the CT images occured during the second stage of the experiment but when comparing the average density values for each slice before and after the pore pressure decrease, an overall negative change is observed. This decrease in density is attributed to a partial dissociaton of methane hydrate during this stage.
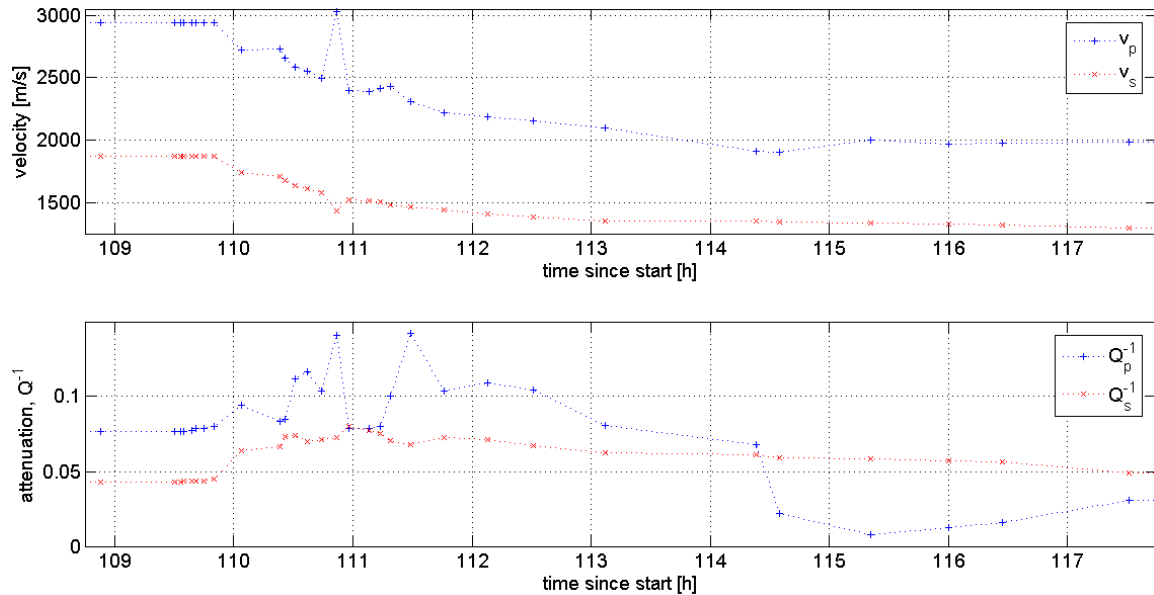
Figure 12. Compressional and shear velocity with pore pressure decrease

Experimental Phase 3: CO_2/N_2 Gas Substitution

A CO_2 and N_2 gas mixture was flowed through the sample at a pore pressure of 9.6 MPa. Young's and shear modulus all show significant increases upon gas injection followed by a decrease due to heating of the sample (Figure 13). Due to the hydrate blockage in the sample, gas hydrate formation is stopped before full conversion of all water and CO_2/N_2 gas in the sample is reached. That results in lower values for Young's modulus and shear modulus than after methane hydrate formation in Phase 1. Both attenuations increase upon gas injection and then periodically increase and decrease with each heating cycle.
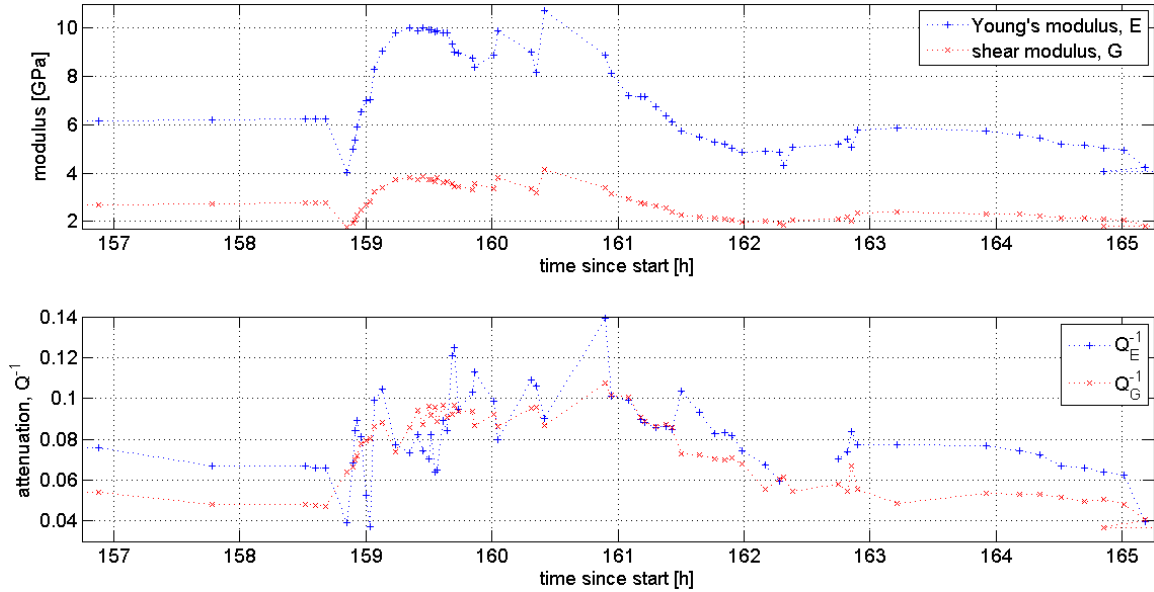
Figure 13. Inverted Young's modulus and shear modulus with corresponding attenuations from SHRB data recorded during partial dissociation of methane hydrate due to CO_2/N_2 injection and temperature changes.

Attenuation of pure hydrates

The purpose of these experiments was to find out how much of the actual attenuation is caused by the hydrate itself. For that reason we performed ultrasonic velocity measurements on pure tetrahydrofuran (THF) hydrates. THF was chosen because of its stochiometric relationship with water. By mixing 19 wt% of THF with 81 wt% of water the mixture should result in a 100 % pure THF hydrate. Also, the THF hydrate stability temperature is above the freezing point of water which means that if there is residual fluid in the system it is in a liquid stage.

Experimental Setup & Procedure

To perform this kind of experiment we designed a sample holder which allows us to measure fluids (Figure 14). It consisted of Tygon tubing in which small holes were drilled. Wires were put through those holes which kept the PEEK end caps in place and at a distance of 2 cm from one another. The end caps contained 500 kHz piezoelectric transducers as well as fluid lines for fluid injection. After the fluids were injected into the sample holder the fluid lines were closed and the sample was submersed into a temperature controlled cooling bath. Ultrasonic P- and S-waves were recorded at room temperature (25° C) as well as at 1 °C and -10 °C. By collecting the waveforms we were able to calculate the ultrasonic velocities by simply dividing the length of the sample by its arrival time. (Note: A dead time and temperature correction had to be performed before calculating the ultrasonic velocities.). Furthermore, the first cycle of the P-wave arrival was analyzed with respect to its frequency content. Ultrasonic attenuation can be calculated by dividing the amplitude spectrum of a standard by the amplitude spectrum of the sample. The

standard used in this study was aluminum. This method relies on the fact the attenuation of the used standard is negligible. For more information see Toksöz et al, 1978.
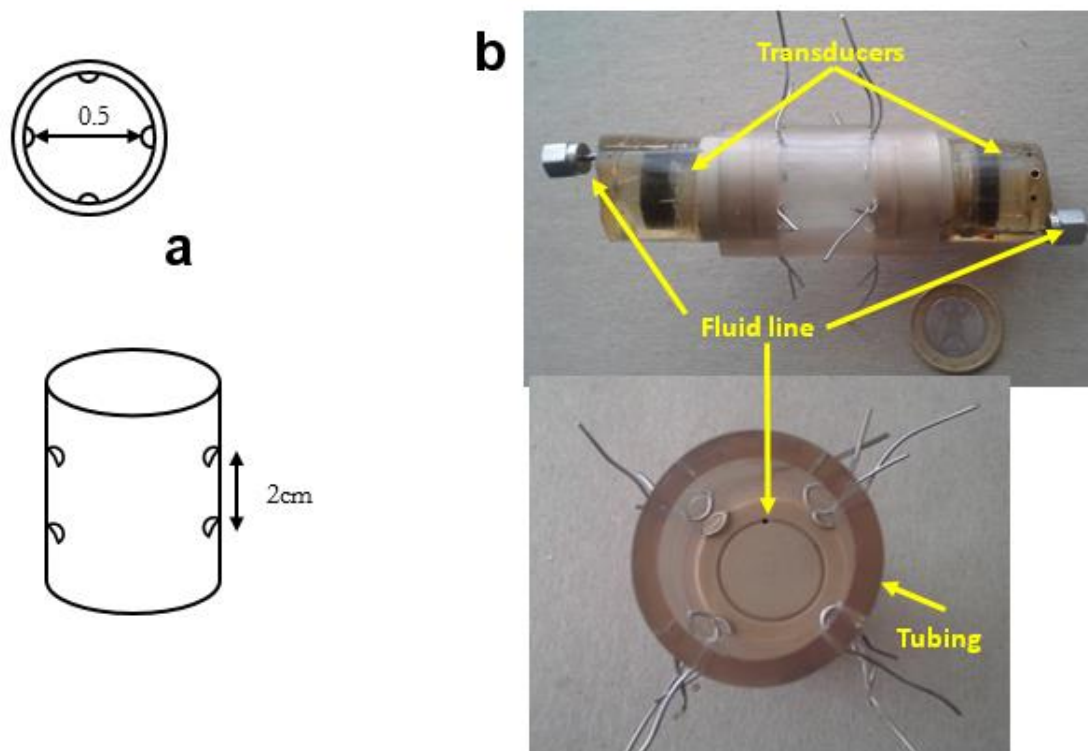
Figure 14. Ultrasonic sample assembly a) Scheme of the sample b) Photograph of the sample holder with transducers.

Results

Figure 2 shows the raw waveforms of the measured samples. The waveforms for the sample only containing water were taken at room temperature. Their corresponding velocities are shown in Table 1. The samples that contained a "100 %" hydrate were taken at 1 °C and are shown in green. It is noticeable that we have a velocity increase by a factor of 2 compared to the water samples. Also the peak to peak amplitude dropped. Cooling the sample further down to -10 °C resulted in another velocity increase as well as an increase in the peak to peak amplitude. This additional increase in velocity suggests that there is residual water in the sample that is now converted into ice causing an additional stiffening of the sample. Even though THF has a stochiometric relationship with water it is almost impossible to mix a mixture that results in 100 % THF hydrate. The reason for that is that THF is extremely volatile and during the mixing process of water and THF some of it evaporates leaving a mixture that results in a sample that

contains excess water after hydrate formation. At last the waveform of the aluminium can be seen in Figure 2. The velocity calculation for its first arrival corresponds with literature values (Internet1).

Using those first arrivals and analyzing them regarding their frequency content is shown in Figure 3. It can be seen that the aluminum standard has much higher frequency content than the samples itself, as expected. Furthermore, the shape of the frequency curves is similar for each set of samples, showing that the measurements, especially for the hydrate bearing case, were reproducible. Now, comparing the peak frequency of the water samples with the frozen samples shows that they are fairly similar and also the shape of the curves show the same frequency content (Figure 3 d). On the other hand the "pure" THF hydrate samples have lower peak frequencies as well as a much faster decay or a lesser amount of higher frequencies in the frequency spectrum. This indicates that the wave propagating through the sample gets attenuated. From the waveforms we already concluded that there is residual water in the sample. This water is the cause of the attenuation that we observed because it is being squirted through the pore space causing a loss in energy (Johnston et al, 1979). However, after freezing the sample, the residual water turns into ice. The fact that the frequency spectrum of water is comparable with the one of the frozen sample is so similar leads to the assumption that the hydrate itself has no to very little attenuation.
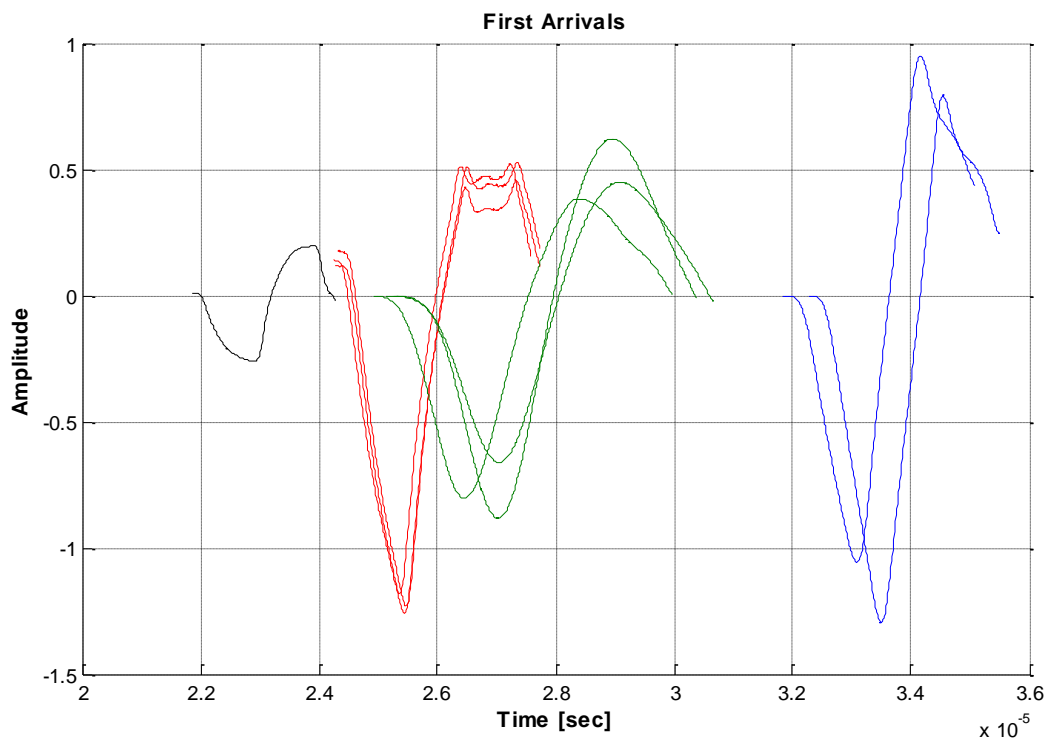
Figure 15: Raw waveforms for the first arrivals for the p-wave, aluminium standard (black), frozen sample (red), only hydrate bearing (green), and water (blue)
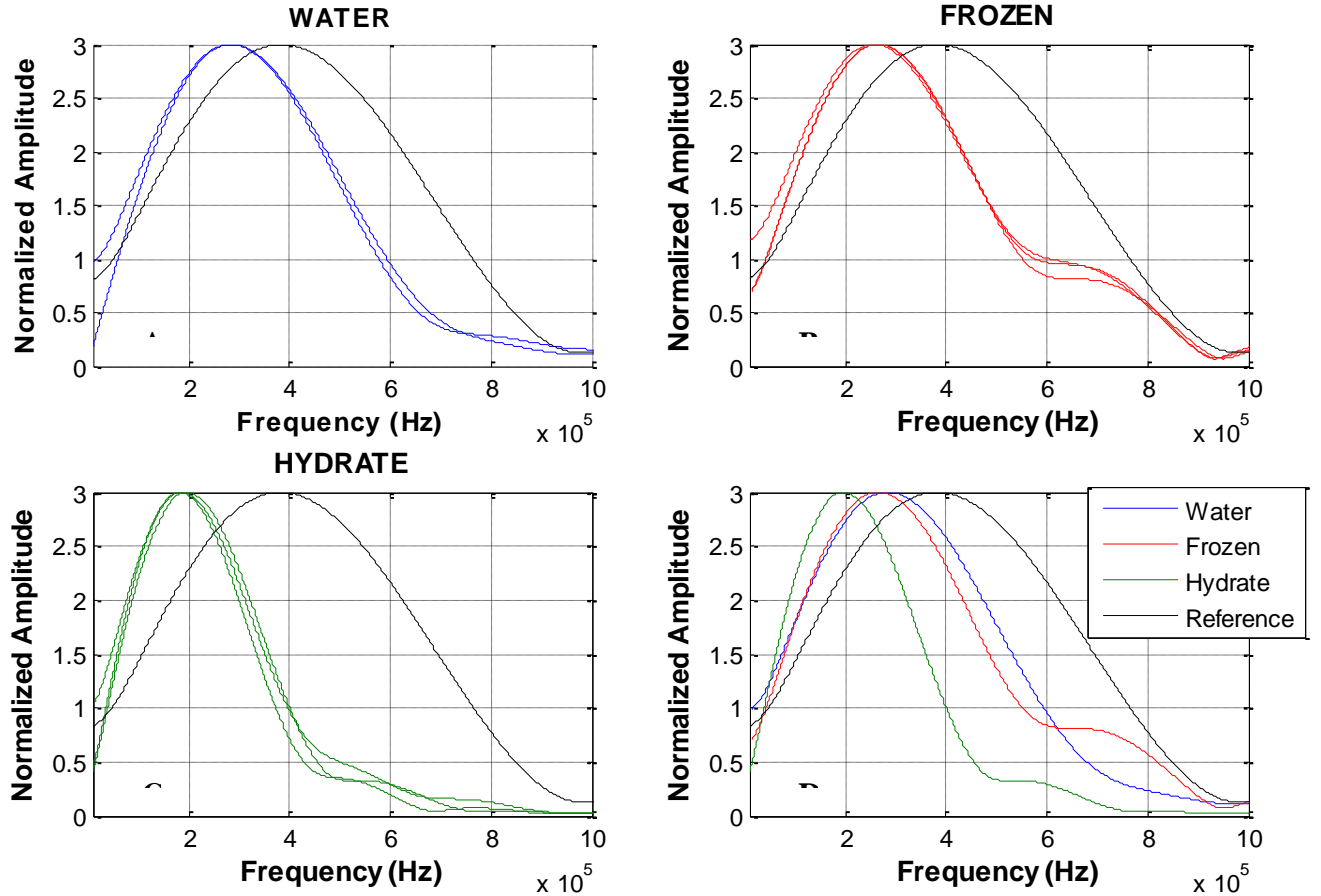
Figure 16: Frequency content of first arrivals. A) Frequency spectrum for water. B) Frequency spectrum for the frozen sample. C) Frequency spectrum for the "100 %" THF hydrate sample. D) Comparison of Water, Frozen, and Hydrate frequencies.

Table 1: Summary of calculated velocities, peak frequencies, and peak to peak amplitudes for all the samples.

Sample	Velocity (m/s)	Peak Frequency (kHz)	Peak-Peak
Water I	1527	285.8	2.0082
Water II	1558	281.1	2.0875
Frozen I	3484	276.0	1.6919
Frozen II	3544	264.1	1.6920
Frozen III	3556	269.9	1.7380
Hydrate I	3257	198.4	1.5037
Hydrate II	3090	183.9	1.1843
Hydrate III	3140	188.1	1.1101
Aluminium	6030	388.1	0.4617

Conclusion on ultrasonics

In summary we were able to perform ultrasonic velocity measurement on fluids. Even though we were not able to form 100 % THF hydrates we were still able to show that the hydrate itself has an almost negligible attenuation. The fact that there was a small amount of water in the hydrate sample caused an observable attenuation due to the squirting effect of the water through the pores which is triggered by the passing wave.

Acknowledgments

Plans

We plan to focus on the same topics as currently described in this quarterly report:

- Continue ultrasonic measurements of attenuation on pure hydrate phases – both THF and methane

- Extend NMR measurements to quantify residual liquid water in samples

- Compare laboratory attenuation measurements with reported in situ data

- Complete installation and calibration of Torlon vessel in CT scanner
      Temperature control
      Pore pressure control

- Convert water/ice into THF and methane hydrate within the CT scanner and document textures.

As we have seen in this quarterly report, attenuations will be strongly dependent on any unconverted water phase remaining in the sample. Both more freezing and use of the Nuclear Magnetic Resonance (NMR) system can help identifying mobile water. The NMR has difficulty identifying very small amounts of liquid water or if it is contained in very small pores or fractures.

Participants and Collaborating Organizations

Name: George Radziszewski
Project Role: Research Faculty
Nearest person month worked this period: 1.5
Contribution to Project: Dr. Radziszewski spent his time establishing standards and procedures for running the MicroCT scanner .
Funding Support: "Organics, Clays, Sands and Shales (OCLASSH) consortium
Collaborated with individual in foreign country: No
Country(ies) of foreign collaborator: N/A
Travelled to foreign country: Yes
If traveled to foreign country(ies): (Poland)
Duration of stay: 3 weeks

Name: Mathias Pohl
Project Role: Graduate Student
Nearest person month worked this period: 3
Contribution to Project: Mr. Pohl prepared samples and collected ultrasonic data.
Additional Funding Support: N/A
Collaborated with individual in foreign country: No
Country(ies) of foreign collaborator: N/A
Travelled to foreign country: No
If traveled to foreign country(ies)
duration of stay: N/A

Name: Mandy Schindler
Project Role: Graduate Student
Nearest person month worked this period: 3
Contribution to Project: Ms Schindler prepared samples and collected CT data.
Additional Funding Support: N/A
Collaborated with individual in foreign country: No
Country(ies) of foreign collaborator: N/A
Travelled to foreign country: No
If traveled to foreign country(ies), (Germany, China)
duration of stay: 2 weeks

Name: Weiping Wang
Project Role: Laboratory Manager
Nearest person month worked this period: 1
Contribution to Project: Mr. Wang assisted in equipment fabrication
Additional Funding Support: Fluids consortium, Chinese Mining University
Collaborated with individual in foreign country: No
Country(ies) of foreign collaborator: N/A
Travelled to foreign country: Yes
If traveled to foreign country(ies), China
duration of stay: 3 weeks

Name: Andrew Markey
Project Role: Student
Nearest person month worked this period: 0 (just started)
Contribution to Project: Andrew will help collect CT data.
Additional Funding Support: 'Fluids' consortium
Collaborated with individual in foreign country: No
Country(ies) of foreign collaborator: N/A
Travelled to foreign country: No
If traveled to foreign country(ies),
duration of stay: N/A

Name: Michael Batzle
Project Role: Principle Investigator
Nearest person month worked: 1
Contribution to Project: Overall (dis)organization.
Funding Support: Academic faculty
Collaborated with individual in foreign country: No
Country(ies) of foreign collaborator: N/A
Travelled to foreign country: N/A
If traveled to foreign country(ies):

Name: Manika Prasad
Project Role: Co-Principle Investigator
Nearest person month worked: 0.25
Contribution to Project: NMR & acoustic measurements
Funding Support: Academic faculty
Collaborated with individual in foreign country: No
Country(ies) of foreign collaborator: Permanent Resident, U.S.
Travelled to foreign country: Y
If traveled to foreign country(ies): India, Norway, Germany, Houston

External Collaborations:
Dr. Tim Collett
US Geologic Survey
Denver, Colorado: (if foreign location list country)

Support: Data and guidance on interpretation and application
Tim continues to publish numerous papers on hydrate properties

Lawrence Berkeley National Laboratory
Hydrate facility
Timothy Kneafsey
Seiji Nakagawa

Changes / Problems

Several factors will occur that might impact the progress of this projects. Both Manika Prasad and Michael Batzle will be on sabbatical leave during the spring of 2015. Both will be returning periodically to supervise students and re(dis)organize projects. However, the graduate students and staff on this project are sufficiently proficient in their research or tasks to perform with minimal supervision. George Radiziszewisky still plans to retire at the end of this year. He has been responsible for much of the CT imaging conducted on our hydrate-bearing sediments. The plan is to utilize Mr. Weiping Wang, our laboratory manager, and student Andrew Markey to perform some of the tasks. In addition, Mr. Radiziszewisky will be working on the project part time starting in March. We will also need to reconcile the project ending dates: I have been planning on project ending December 31, 2015 (see Table 2); but close inspection of contract gives an ending date of September 31, 2015.

Special Reporting Requirements

None

Budgetary Information

Attached separately

References

Dvorkin, J, R. Uden (2004), "Seismic wave attenuation in a methane hydrate reservoir" The Leading Edge Interpreter's Corner

Guerin, G., and Goldberg, D., 2002. Sonic waveform attenuation in gas hydrate–bearing sediments from the Mallik 2L-38 research well, MacKenzie Delta, Canada. J. Geophys. Res., 107:2088. doi:10.1029/2001JB000556

Hester, K. C., and Brewer, P. G., 2009, Clathrate hydrates in nature.: Annual review of marine science, 1, 303-27.

Johnston, D.H. ,M. N. Toksöz, and A. Timur (1979), Attenuation of seismic waves in dry and saturated rocks: II Mechanisms, Geophysics, 44, 691,

Nakagawa, S., 2011, Split Hopkinson resonant bar test for sonic-frequency acoustic velocity and attenuation measurements of small, isotropic geological samples.: The Review of scientific instruments, 82, no. 4.

Pratt, R.,K. Bauer, and M. Weber (2003), Crosshole waveform tomography velocity and attenuation images of arctic gas hydrates, paper presented at 73rd Annual Meeting, Soc. Of Explor. Geophys., Dallas, Tex.

Schoderbek, D., Martin, K. L., Howard, J., Silpngarmlert, S., and Hester, K., 2012, OTC 23725 North Slope Hydrate Field trial : CO_2 / CH_4 Exchange:, , no. December 2011, 1-17.

Sloan, E. D. & Koh, C. A. (2008), Clathrate Hydrates of Natural Gases. 3rd ed., CRC Press, Taylor & Francis Group, Boca Raton, FL

Toksöz, M.N., Johnston, D.H., and Timur, A., 1978, Attenuation of seismic waves in dry and saturated rocks: 1. Laboratory measurement; Geophysics, 44, 681-690.

Wood, W.T., Holbrook, W.S. & Hoskins, H., (2000), "In situ measurements of P-wave attenuation in methane hydrate and gas bearing sediments on the Blake Ridge" Proc. ODP. Results, Vol 164, pp. 265-272, eds Paull, C., Matsumoto, R., Wallace, P. & others, Ocean Drilling Program, College Station, Texas

Internet1:   http://www.trinityndt.com/brochures/Ultrasonic_Inspection_Velocity_Table.pdf 10/23/2014 14:11

Milestone Status

Our current position on the time chart is shown in Figure 17. We are approximately at the halfway mark of the project, and we are perhaps slightly behind schedule. At this point, we have should be proficient, but currently we have formed only small amounts or relied on external facilities.
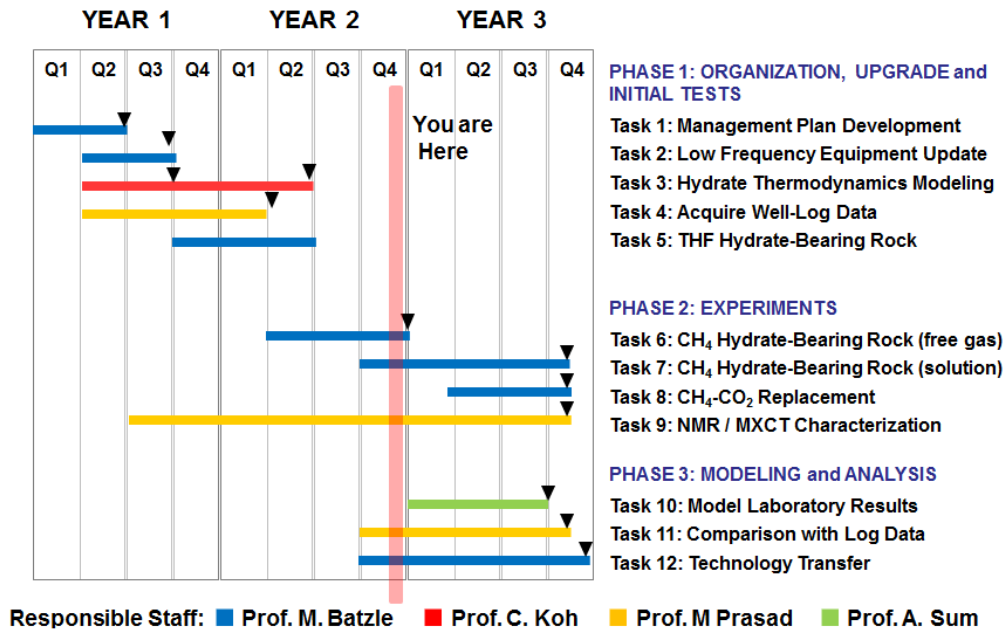

Figure 17. Milestone Status. We are at the end of our seventh quarter and are approaching the start of the final phase of this project.

Table 2. Milestone status

Measurement and Interpretation of Seismic Velocities and Attenuations in Hydrate-Bearing Sediments
DOE Award No.: DE-FE 0009963

Milestone Title / Description		Status	Completion date (completed or expected)
Completed:			
1	Project Management Plan (PMP)	Complete & approv..	1 Dec 2012
2	Modifications to low frequency system	Completed	1 Jun 2013
3	Modeling established using EOS	Completed	31 May 2014
4	Property models of hydrates completed	Completed	31 May 2014
5	Logs acquired and database estab.	Completed	15 Jun 2014
6	THF hydrate grown in pressure vessel	Completed	15 Apr 2014
7	Methane hydrates from free gas phase (somewhat behind schedule)	Continuing*	31 Dec 2014
Continuing or Planned			
8	Methane hydrates from gas in solution	Planned	30 Jun 2015
9	CO_2 replacing methane in hydrates	Planned	30 Sep 2015
10	MXCT scans conducted	Continuing*	30 Sep 2015
11	Effective media models complete	Planned	30 Sep 2015
12	Comparison to in situ data complete	Planned	15 Oct 2015
13	Information Dissemination	Continuing*	31 Dec 2015

*initial stages were completed on schedule, but the process continues throughout the project